Lawrence Livermore National Laboratory

PROGRAM UPDATE - JANUARY 2002

Laser Science & Technology

Dr. Lloyd A. Hackel, Program Leader

UCRL-TB-136126-02-1

LS&T Improves CO_2-Laser Treatment of NIF Final Optics

A limitation to the performance of high-fluence laser systems is the growth of small damage sites on exposure to subsequent laser pulses. Even state-of-the-art production methods yield a small number of initiator sites that would be expected to grow on exposure to high fluence. Previous work has shown that treatment with a CO_2 laser can prevent damage from growing.

The CO_2-laser treatment process has been improved, and significant steps have been taken towards implementing the technique in a production facility (Figure 1). The key to the improvement is the minimal-vaporization technique applied to small initiators before they experience significant growth. A low-power (~2.5 W CW), tightly focused (~125 µm diameter) CO_2 laser beam, with an exposure time of ~10 ms, has been used to treat these small initiators. The resulting pit is only ~75 µm diameter and 1 µm deep. These treated sites do not grow further when exposed to 350-nm pulses at ~14 J/cm^2 and a few ns duration.

Treatment of optical damage with a CO_2 laser is expected to play a central role in the life cycle of National Ignition Facility (NIF) fused-silica optics in the Final Optics Assembly (FOA). Figure 2 shows two separate input streams into the CO_2 treatment cycle during the material flow of optics from initial production at the vendor to scrap at the end of the useful life. The upper stream, shown in black, represents the final treatment of optics prior to installation. The CO_2 treatment cycle identifies these sites while they are still small and modifies them so they will not grow. This process is the focus of the current work.

The lower stream, shown in red, represents optics with identified damage removed from the system.

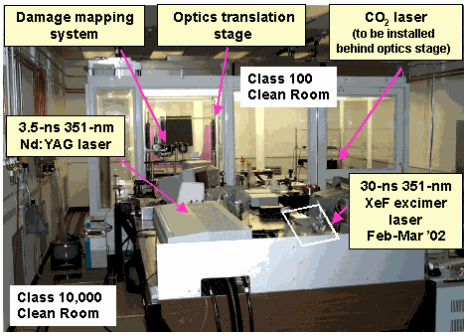

Figure 1. The Phoenix conditioning and mitigation facility.

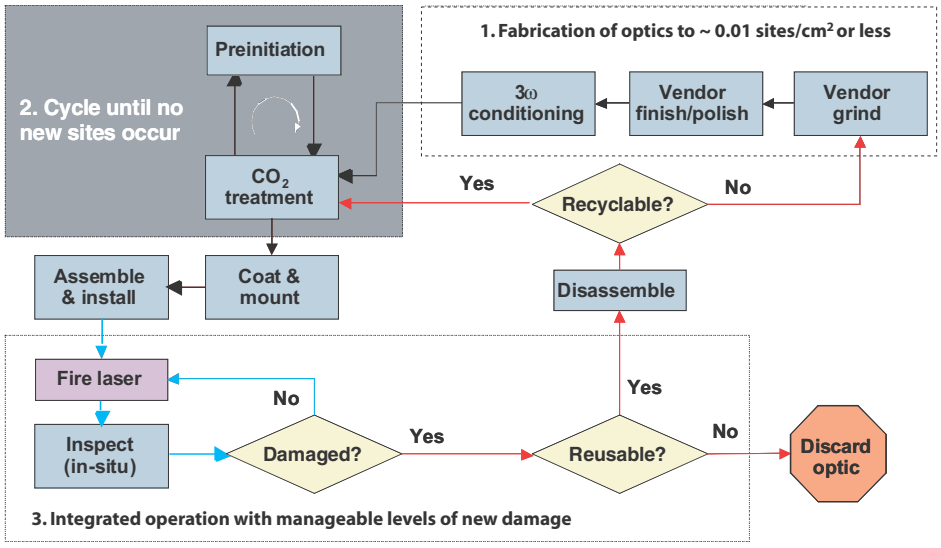

Figure 2. Material flow for NIF FOA fused-silica optics. Shaded region represents CO_2 mitigation process.

Some sites eventually damage during operation. Although the mitigation of these larger sites will leave larger and deeper pits, CO_2 treatment can halt further growth of these sites.

Key to implementing the mitigation process are four critical components: (1) The required parameters for the CO_2 laser treatment must be determined. This includes not only determining how to treat damage sites so that they no longer grow when exposed to high fluence 350-nm light, but also ensuring that the resulting modification of the surface does not lead to damage of downstream optics due to beam modulation. (2) Small damage sites must be located and targeted. (3) A process must be developed that ensures that all damage precursors have been mitigated. (4) The process must be automated to deliver the high throughput required for NIF. Progress has been made in each of these key areas.

Figure 3 shows two of the sites that have been successfully treated. Of the approximately 60 naturally initiated sites that have been mitigated, only one grew when exposed to 14-J/cm^2 fluence of 350-nm light. This one failure is probably the result of an alignment problem. Measurements of the diffraction patterns of the mitigated sites have shown relatively small peak beam modulation extending over only a small area. The modulation usually peaks within a few centimeters of the treated site and then falls. Work is continuing to study the effect of modulation on downstream damage.

Progress on implementation and automation of the process has also been made. Production of very small mitigation sites requires tight alignment tolerances and a short depth-of-focus which increases the complexity in the treatment of curved optical surfaces. An alternative to maintaining tight tolerances is using slightly larger mitigation sites that still have acceptable beam modulation properties. Mitigation sites two or three times larger (~50 µm) may be an acceptable tradeoff. A new facility will be activated in February to develop the automation and integration capabilities required for production of 3ω optics for NIF. This technique will help to ensure reliable operation of NIF final optics.

—William Molander

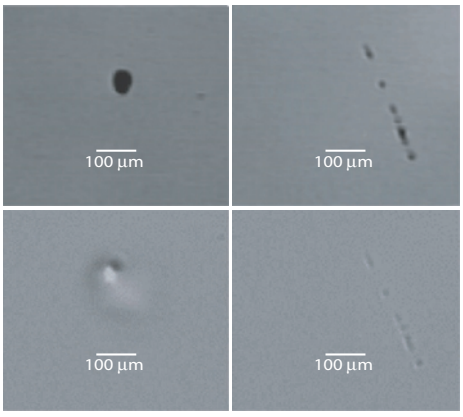

Figure 3. Microscope images of two damage sites before (top) and after (bottom) CO_2-laser treatment. These sites were created in a raster scan at 14 J/cm^2. After mitigation there was no further growth at 14 J/cm^2.

For comments about content of the *LS&T Program Update*, contact Dr. Hao-Lin Chen (925) 422-6198.
To get on the mailing list of the *LS&T Program Update*, send a request to Louann Arredondo, arredondo1@llnl.gov

This work was performed under the auspices of the U.S. Department of Energy by University of California Lawrence Livermore National Laboratory under Contract No. W-7405-Eng-48.

Lawrence Livermore National Laboratory,
Livermore, California

Program Update - February 2002

Laser Science & Technology

Dr. Lloyd A. Hackel, Program Leader

UCRL-TB-136126-02-02

Laser Peenforming—A New Precision Metal-Forming Technology

In a collaborative effort with Metal Improvement Co. Inc., of Paramus, N.J., we are evaluating the effectiveness of laser peenforming to precisely form metal panels for aerospace and defense applications. Using a kilowatt-class pulsed Nd:glass laser, we are able to selectively place residual compressive stress into the surfaces of thick metal panels to form them into precise and complex shapes without yielding the metal and leaving both surfaces in crack-resistant compressive stress state.

Similar to the laser peening process originally developed for increasing fatigue and corrosion resistance of metals, the peenforming technique, recently developed by LS&T, uses a high-energy and high-intensity solid-state laser to impress a deep level of residual stress into selected surfaces of the metal. The strain associated with the compressive residual stress causes the treated surface to elongate, effectively curving the metal within the peened area. By optimizing the process parameters such as laser fluence (~100 J/cm^2), intensity (5 to 10 GW/cm^2), and number and location of treatment pulses, we are able to precisely form a broad range of aluminum alloys to contours and shapes that could not be adequately made using conventional methods.

Figure 1 shows three aerospace-grade 2024-T-3 aluminum alloy plates 1 in., 3/4 in., and 5/8 in. thick formed by the laser peenforming technique. We were able to form them to precise curvatures and bend radius by adjusting the laser peening parameters and peening location. We have also formed a 5/8-in.-thick aluminum plate (Figure 2) into a precise saddle shape with 150-in. radius of curvature, concave and convex on alternating surfaces.

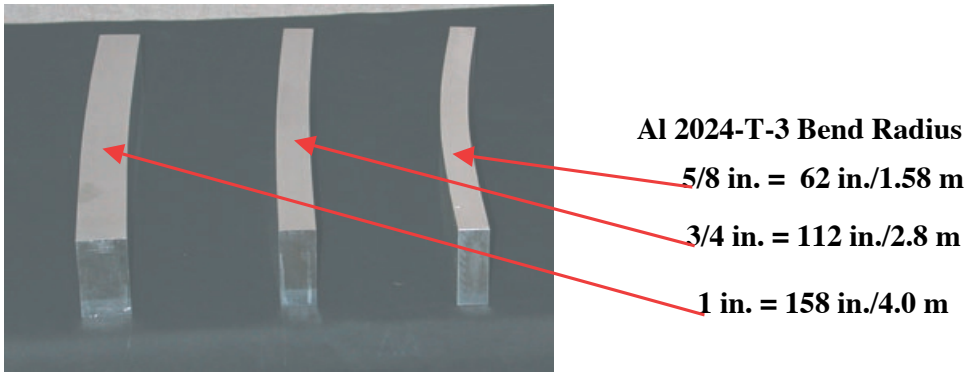

Figure1. Thick aluminum metal sections have been formed by laser peenforming without yielding the metal and leaving both surfaces in a crack-resistant compressive stress state.

Forming is critically important to the fabrication of structural wing skins for large commercial and military aircraft. Many components on aircraft such as wing skins, elevator and rudder panels, and winglets need to be formed to precise complex curvatures both to meet aerodynamic requirements and to fit precisely on the airframe for stress-free fastening. These structural components cannot be bent using conventional hydraulic or other force forming techniques because bending causes undesirable yielding of metal. Metal yielding causes loss of mechanical strength and always leaves surfaces in tension, thus susceptible to fatigue fracture and corrosion cracking. In the past, the aerospace industry has used an iterative forming process (repeated mechanical shot peening and thermal age creeping) to form and shape metal panels. This iterative process works well but is limited to only 7000 series aluminum to which age creep forming can be applied. The process is not precise, and parts have to be repeatedly treated and checked in a forming jig until the fit meets specification. Using laser peenforming, one could potentially make the 40-meter outer skin of an airplane wing fit precisely onto its frame with just one or two treatments.

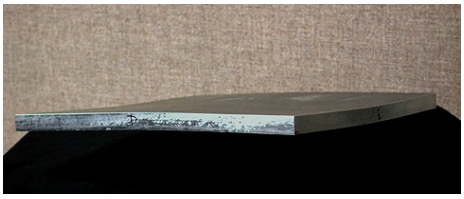

Figure 2. A 5/8-in.-thick 2024 T-3 aluminum plate formed to a saddle shape by laser peenforming. Laser peenforming can form metal panels with complex curvatures.

The laser peenforming process will dramatically change aircraft manufacturing in terms of cost and efficiency as well as the introduction of a new capability for designing and forming of metal components. The ability to form large structural members using lighter-weight panels and fewer joints can significantly reduce aircraft weight and increase payload and fuel efficiency. We are working closely with industry to commercialize this technology.

—Lloyd A. Hackel

For comments about content of the *LS&T Program Update*, contact Dr. Hao-Lin Chen (925) 422-6198.
To get on the mailing list of the *LS&T Program Update*, send a request to Frances Mendieta, mendieta1@llnl.gov
This work was performed under the auspices of the U.S. Department of Energy by
University of California Lawrence Livermore National Laboratory under Contract No. W-7405-Eng-48.

Lawrence Livermore National Laboratory
Livermore, California

PROGRAM UPDATE - MARCH 2002

Laser Science & Technology

Dr. Lloyd A. Hackel, Program Leader

UCRL-TB-136126-02-03

Compact Microchannel-Cooled Laser-Diode Arrays Deliver over Tens of kW/cm² onto the Working Surface

Last year we reported the delivery of a 41-kW-peak-power diode array module constructed using LLNL Silicon Monolithic Microchannels (SiMMs) packages. In total, four of these modules (one of which is shown at right) are being delivered to the Solid-State Heat-Capacity Laser Project for optical pumping of a high-average-power solid-state laser. These initial modules are being used for characterization and testing of a subscale laser slab.

As reported earlier (see November 2001 *LS&T Program Update*), the SiMMs module brings unsurpassed average radiance (or brightness) capability to laser-diode arrays. This performance is attained through a unique combination of microscopic cooling channels in a silicon substrate that serve to remove waste heat, and precision microlenses that serve to condition the output radiation from the laser-diode bars that are mounted on the package (see pictures at bottom of columns 1 and 2). The use of silicon as the solid material in the heat-conducting portion of the SiMMs package is critical. It makes possible the fabrication of thousands of tiny (~30-μm-wide) cooling microchannels in very close proximity to the heat-producing laser-diode bar arrays. The use of silicon also makes possible the precision location of multiple bars on a single substrate, allowing an array of precision-located cylindrical microlenses to be attached in a single step.

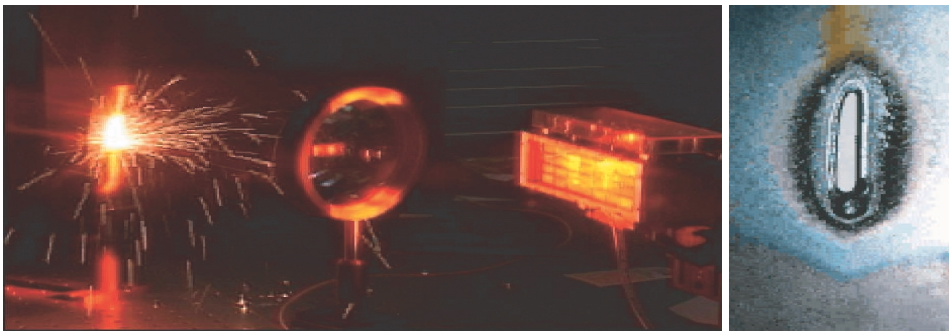

On the left is a 41-kW peak power SiMMs diode array operational with its output radiation focused onto a steel plate. This diode array is constructed from 28 closely packed SiMMs tiles. On the right is the hole that was burned through the steel plate.

Optimizing the performance of laser-diode bars was one of the primary considerations in the design of the SiMMs package. The aggressive cooling capability of the SiMMs package enables efficient operation of laser diode arrays in a very tightly packed geometry. The peak electrical efficiency of a SiMMs package is about 48%, converting nearly half of the electric input power into light output. Average exitance from the SiMMs laser-diode arrays operating in a CW mode is up to be 600 W/cm², which is ~3 times higher than available today. With microlens conditioning, the output radiation from a SiMMs package is confined to an angular region of 6° by 0.6°, giving an unsurpassed average radiance capability of ~0.5 MW/cm²-steradian. This technology is available for transfer to interested commercial enterprise.

Initial testing of the laser modules is focused on characterizing pump light delivery efficiency and pump light uniformity delivered onto the Nd:GGG laser disks that comprise the gain medium of the heat-capacity solid-state laser. Part of this testing involves characterizing the radiation emitted by the modules. The figure at top right shows the result of one test in which the output radiation from the module was focused onto a stack of steel plates having total thickness of 3 mm. After a brief exposure of ~5 s, a narrow slit (approximately 4 mm × 35 mm) was produced. During this exposure, the diode array was operated at a 10% duty factor (500-μs pulse width and 200-Hz pulse repetition frequency) and developed a peak power of 41 kW. The average power density at the focal spot on the steel plates during this test was estimated to be ~3 kW/cm². During the coming year, we plan on building a three-slab sub-module of the ultimate 100-kW system. This sub-module will use a total of 12 diode backplanes whose size will be twice what is currently used (56 ten-bar tiles per backplane). The total amount of peak diode power will be approximately 1 MW.

Besides optical pumping of solid-state lasers, we are also evaluating possible applications of SiMMs modules to welding and surface treatment of materials. Areas of particular interest are brazing, heat-treatment, and surface hardening of metals. These material processing applications directly benefit from our SiMMs packaging technology because of the high irradiance—upwards of tens of kW/cm²—that can be delivered to the working surface of samples. The SiMMs package represents a significant breakthrough in high-power diode-array packaging technology and enables the scaling of power from 2-D diode arrays to 100 kW or larger with extremely high brightness. Currently 840-kW arrays are in production for the heat-capacity laser program. When completed, these will be the most powerful average-power diode arrays in existence.

—R. Beach, B. Freitas, and M. Rotter

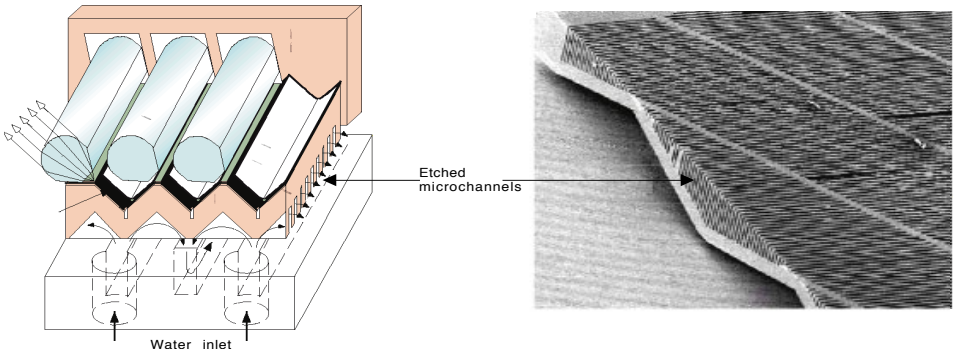

On the left is a cutaway sketch of a SiMMs package showing the location of the microchannels, which are fabricated into the silicon top layer of the package. On the right is an SEM photograph of a silicon wafer used in the SiMMs production showing the 30-μm-wide microchannels for cooling water that are fabricated using photolithography and anisotropic etching.

For comments about content of the *LS&T Program Update*, contact Dr. Hao-Lin Chen (925) 422-6198.
To get on the mailing list of the *LS&T Program Update*, send a request to Frances Mendieta, mendieta1@llnl.gov

Lawrence Livermore National Laboratory
Livermore, California

PROGRAM UPDATE - APRIL 2002

Laser Science & Technology

Dr. Lloyd A. Hackel, Program Leader

UCRL-TB-136126-02-04

Beam Sampling Gratings for Power Measurement and Balance of NIF Beams in Fabrication

Balancing the power on all the National Ignition Facility (NIF) beams requires a precise power measurement on each individual beam. This measurement has to be stable to ±1% over a period of time and should be directly relatable to the energy on target without additional ambiguities or uncertainties. This requires that the measurement be done as close to the end of the laser chain as possible. Using a Fresnel reflection off an optical surface does not provide the required stability because the antireflection coatings degrade over a period of time.

A transmissive diffraction grating inserted in the beam path provides a stable sample of the beam for the power measurements. The requirements on this beam sampling grating (BSG) for NIF are that the grating diffract a small fraction (~ 0.2%) of the incident high-power laser beam and bring it to focus at a distance of approximately 1.2 m from the optic. This requires a shallow grating structure (~15 nm deep) with concentric grooves as shown schematically in Figure 1. The grating period ranges from 1 to 3 μm.

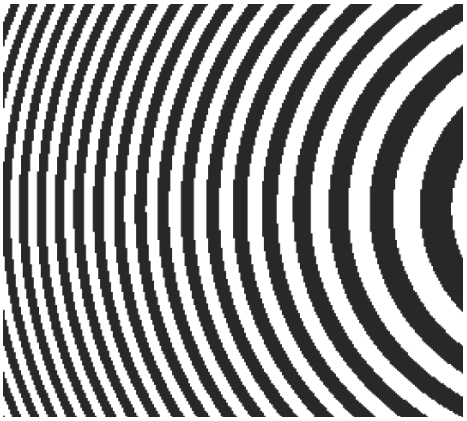

Figure 1. Schematic of the beam sampling grating (BSG) groove profile.

Figure 2. Beam sampling grating patterning station.

Figure 3. Automated wet-processing machine for beam sampling grating production.

We use interference lithography to fabricate the beam sampling gratings. The exposure system for fabricating the beam sampling gratings is shown in Figure 2. Here a layer of photoresist deposited over the fused silica substrate is exposed to the interference pattern of two diverging beams at 351 nm originating from the main focus and the sampled focus. After exposure, the exposed photoresist is developed off, leaving photoresist grooves separated by clear areas. At this stage, we transfer the grating pattern into the fused silica substrate by etching clear areas using a buffered hydrofluoric acid solution. Finally the remaining resist is washed off, leaving a clear fused silica optic with ~15-nm-deep grating profile. The automated wet-processing machine for BSG production is shown in Figure 3.

Figure 4 illustrates the operation of a 40-cm-aperture beam sampling grating. Here the grating is illuminated with a white-light source (hidden behind the screen), and the converging and the diverging diffracted orders are seen on the screen past the grating.

A wet-chemical processing machine and a patterning-and-illumination station were assembled to fabricate full-size BSGs with 5- to 30-nm groove depth for damage testing in NIF. We completed building and testing of production hardware for fabricating NIF BSGs that will be used to perform critical power balance of the 192 NIF beamlines. We are currently fabricating full-aperture BSGs for NIF to be used on NIF early light.

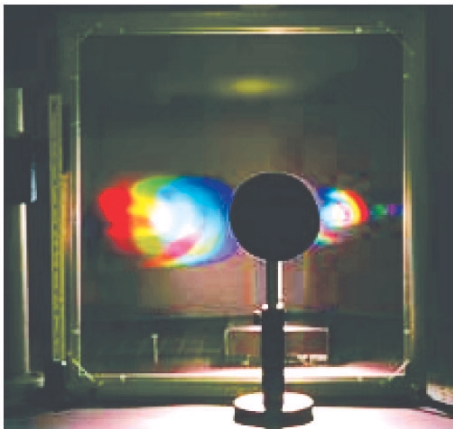

Figure 4. A 40-cm-aperture BSG prototype in operation. A white-light source located behind the black circle in the center of the picture illuminates the grating. The converging and the diverging diffracted orders are seen at the screen located behind the optic.

—S. Dixit, J. Britten, and J. Yu

For comments about content of the *LS&T Program Update*, contact Dr. Hao-Lin Chen (925) 422-6198.
To get on the mailing list of the *LS&T Program Update*, send a request to Frances Mendieta, mendieta1@llnl.gov
This work was performed under the auspices of the U.S. Department of Energy by
University of California Lawrence Livermore National Laboratory under Contract No. W-7405-Eng-48

Lawrence Livermore National Laboratory
Livermore, California

PROGRAM UPDATE - MAY 2002

Laser Science & Technology

Dr. Lloyd A. Hackel, Program Leader

UCRL-TB-136126-02-05

Short-Pulse, High-Average-Power Laser System for Micromachining

Under a work-for-others contract, LS&T is developing a 100-W-class psec, kHz, solid-state laser system for rapid, precision machining of 100-μm-scale features in metals and alloys. This advanced laser drilling (ALD) system has recently been assembled and has undergone initial testing. It delivered, for material processing application, over 50 W in a 2-psec, 4-kHz pulse train to the workpiece.

This short-pulse, high-average-power laser employs numerous advanced laser technologies of the LS&T program. These technologies include a solid-state regenerative amplifier and a power amplifier using diode-pumped Yb:YAG as gain medium and a high-power multilayer dielectric grating. A simplified schematic of this laser is shown in Figure 1. The laser system architecture is based on chirped-pulse amplification (CPA). It starts with a mode-locked Yb-doped fiber laser, which was developed by Imra Corporation specifically for this application. This mode-locked oscillator produces a 4-kHz train of 8-psec, chirped pulses with an average power of 120 mW (2.4 nJ/pulse at 50 MHz). The spectral bandwidth of the oscillator pulses is 2 nm. The psec pulses from the fiber oscillator are stretched in time to 4 nsec using a diffraction grating pulse stretcher, amplified by 75 dB, then recompressed to 2-psec duration before being sent to the target chamber. Between each of these laser subsystems, computer-based pointing and centering loops are used to precisely control laser beam alignment.

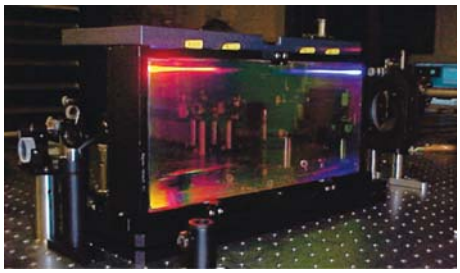

Figure 2. The large dielectric diffraction grating for the ALD laser has a diffraction efficiency of 97% and an rms wavefront of 1/40th of a wave averaged over the surface.

The stretching-and-compressing process that is the basis of the CPA architecture is accomplished by using a high-efficiency dielectric diffraction grating (see Figure 2) manufactured by LS&T's Diffractive Optics Group. This large (150 × 335 mm) multilayer dielectric grating has a diffraction efficiency of >97% at 1030 nm. Whereas a typical CPA-based laser system architecture may use 4 diffraction gratings (2 for the stretcher and 2 for the compressor), the current design employs a single grating that is shared by both the stretcher and compressor. This single-grating stretcher/compressor design enabled the combination of two laser subsystems in a compact unit that can readily be incorporated into a hardened system that can withstand the harsh conditions on the factory floor.

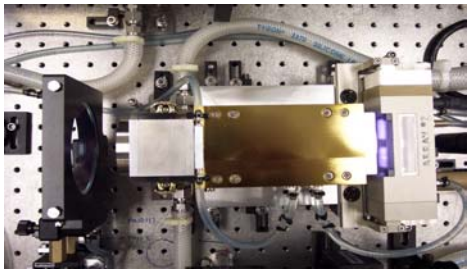

Figure 3. The Yb-YAG amplifier uses LS&T technologies: tapered Yb-YAG rods with heat-diffusing end caps; hollow lens duct; repass pump mirrors; and a water-cooled jacket for the rod.

The 75 dB of amplification between the pulse stretcher and compressor is accomplished by two subsystems: a linear-cavity regenerative amplifier (regen) and a power amplifier. Both amplifiers use Yb:YAG as the gain medium, pumped with microchannel-cooled diode laser arrays (operated at 940 nm). The regen amplifies the 1-nJ stretched-pulses up to 750 μJ and converts the pulsing frequency from 50 MHz to 4 kHz (using a Pockels cell). The power amplifier has two heads. It boosts the regen output from 3 W to 50 W in two passes. With the use of a grating compressor, the pulse width of the amplified beam from the power amplifier is compressed from 2 ns back to 2 psec, multiplying the laser peak power by a factor of a thousand. We developed special water-cooled housings for the amplifier rods to efficiently dissipate heat and minimize amplified stimulated emission and parasitic losses in the laser cavity. The Yb-doped rods are also tapered to minimize parasitic oscillation. Undoped end caps are fused onto the end of each amplifier rod to minimize thermal gradients on the rods. A water-cooled hollow lens duct with precisely machined inner surfaces is used to efficiently couple pump light into the laser rods. Figure 3 shows the power amplifier assembly.

For material processing, the output from the compressor is delivered directly to the workpiece in the target chamber. We have made good progress in the machining of ~100-μm features in metals and alloys as required by our industrial partner. We plan to transfer this high-average-power, solid-state laser technology to our industrial partner for applications in manufacturing.

—J. Crane, G. Huete, L. Shah, M. Shirk, B. Stuart, and S. Telford

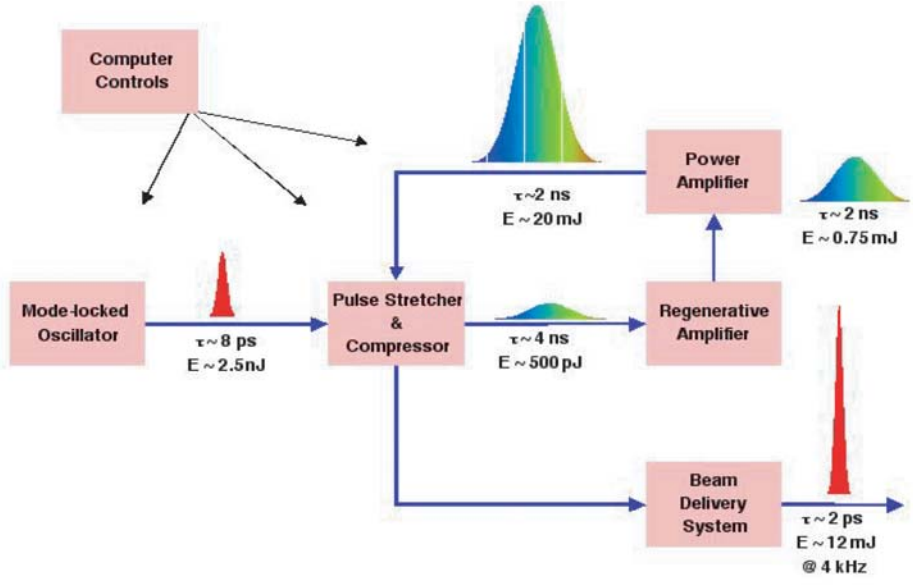

Figure 1. Laser system architecture uses chirped-pulse amplification to produce mJ-level short-pulse output.

For comments about content of the *LS&T Program Update*, contact Dr. Hao-Lin Chen (925) 422-6198.
To get on the mailing list of the *LS&T Program Update*, send a request to Frances Mendieta, mendieta1@llnl.gov
This work was performed under the auspices of the U.S. Department of Energy by
University of California Lawrence Livermore National Laboratory under Contract No. W-7405-Eng-48.

Lawrence Livermore National Laboratory
Livermore, California

PROGRAM UPDATE - JUNE 2002

Laser Science & Technology

Dr. Lloyd A. Hackel, Program Leader

UCRL-TB-136126-02-06

Phase-Locked, Antiguided Multiple-Core Ribbon Fiber Laser

Under the support of the Laboratory Directed Research & Development Program (LDRD) and U.S. Air Force Research Laboratory (AFRL), Albuquerque, N. M., we are developing a scalable multiple-core ribbon fiber laser to generate short-pulse, high-average-power (kW-scale) coherent light for possible applications in the military, material processing, and x-ray generation.

The development of double-clad fiber has brought fiber lasers to the forefront of possible approaches for high-beam-quality, high-average-power laser sources. Using a cladding-pumped geometry with a single-mode core, individual fibers have been demonstrated to yield greater than 100 W of average power. However, it is difficult to increase the outputs of these single-core fiber lasers to higher levels because of the onset of optical facet damage and deleterious nonlinear optical interactions at high irradiance. Critical to increasing the average power capability of fiber lasers is enlarging the aperture area of the laser radiation emerging from the fiber. One way to increase the aperture available to the laser radiation is to employ multiple cores that are phase-locked to yield a coherent output beam. The conventional power scaling techniques using evanescent coupling have not been very successful because of phase fidelity degradation between distant cores in large-diameter fibers.

During the course of this work, we successfully developed a new method to phase-lock multiple fiber cores in a fiber structure via radiative coupling (not evanescent coupling).

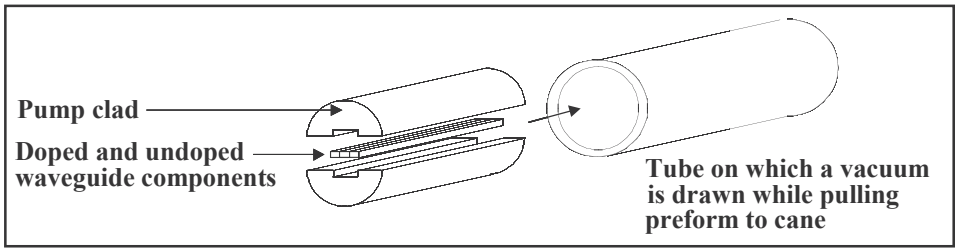

Figure 2. Sketch illustrating the rod-in-tube fabrication technology used to construct the preform for the prototype fiber shown in Figure 1.

This new method, known as antiguiding, which utilizes gain elements radiatively coupled in a "leaky" waveguide array, is analogous to the scheme used earlier for phase locking of laser diode elements. By selective placement of gain regions within a uniform index core, we were able to create a preferred single mode in the fiber. Because the light field is evenly distributed across all cores in this scheme and all gain cores communicate with each other, we anticipate that the scalability of the device will be very favorable.

A cross-sectional view of the prototype Ribbon laser is shown in Figure 1. The waveguide region is rectangular in shape and is comprised of a periodic sequence of gain and no-gain segments having nearly uniform refractive index. It is embedded in a lower-refractive-index cladding region used for diode pumping. Using an end-pumping geometry in which an 808-nm diode array served as the pump source, we were able to run the Ribbon laser predominately in two antiguided modes, as predicted by our modeling.

Figure 2 illustrates the novel "rod-in-tube" fabrication technique that was used to construct the preform for the prototype ribbon fiber. The same technique shows great promise in being able to scale to substantially higher-power-capability fibers.

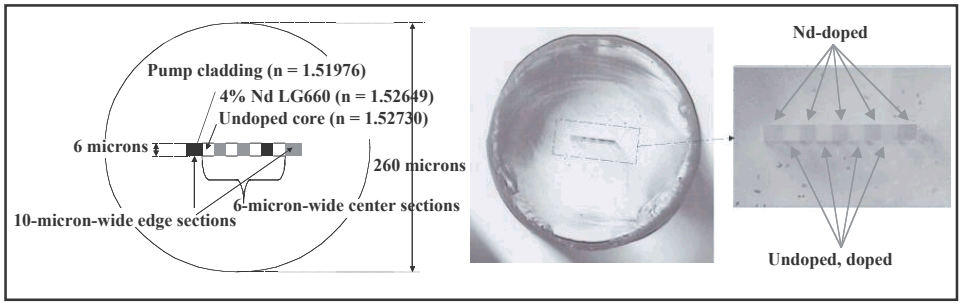

Figure 1. Sketch and photograph of LS&T's prototype five-core Nd fiber in which multiple-gain cores were phased using an antiguiding mechanism.

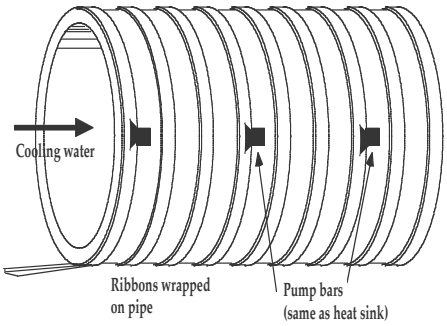

Figure 3. Conceptual design of 30-kW ribbon fiber laser in which a cooled mandrel is used for thermal management, and pump excitation light from diode bars is introduced into the side of the structure.

By using antiguiding mechanism, we successfully demonstrated phase-locking in a five-core Nd-doped glass prototype structure that was fabricated using a novel soft glass fabrication technology. Due to the delocalized nature of their eigenmodes, antiguided structures similar to the ribbon fiber reported here are being evaluated as potential routes to extremely high-power, single-spatial-mode radiation. As an example of a power-scaled system, Figure 3 shows a conceptual design for a 30-kW ribbon fiber. By scaling from 5 cores to 100 cores with fused silica, it should be possible to achieve 30 kW from a single fiber. Achieving this power in laser weapons would be truly revolutionary for the military and, moreover, would have an enormous economic impact in laser material processing and x-ray generation.

—R. Beach, M. Feit, and S. Payne

For comments about content of the *LS&T Program Update*, contact Dr. Hao-Lin Chen (925) 422-6198.
To get on the mailing list of the *LS&T Program Update*, send a request to Frances Mendieta, mendieta1@llnl.gov
This work was performed under the auspices of the U.S. Department of Energy by
University of California Lawrence Livermore National Laboratory under Contract No. W-7405-Eng-48.

Lawrence Livermore National Laboratory
Livermore, California

PROGRAM UPDATE - JULY 2002

Laser Science & Technology

Dr. Lloyd A. Hackel, Program Leader

UCRL-TB-136126-02-07

First Light From the Mercury Laser: a Diode-Pumped, Solid-State, Gas-Cooled Laser for Fusion Energy Applications

Diode-pumped solid-state lasers are one of four driver technologies being considered for inertial fusion energy systems. The competing technologies include heavy ions (Lawrence Livermore National Laboratory, Lawrence Berkeley Laboratory), Z-Pinch (Sandia) and KrF (Naval Research Laboratory). Each driver development program is currently focused on demonstrating several proof-of-principle design concepts.

Mercury is designed to be a 100-J, 10-Hz, 10% efficient prototype laser system, scalable to a 1-kJ aperture with minimal beamline reengineering. To achieve this goal, we explored numerous gain materials and architectural options to best fit the design space of a fusion energy class laser. $Yb^{3+}Sr_5(PO_4)_3F$, called Yb:S-FAP, was chosen as the gain medium based on its long energy storage lifetime, moderately high cross section, and good thermal conductivity.

The primary challenge has been in growing full-aperture slabs of 4x6 cm^2 in area. This past year, we developed a successful growth process to produce half-size slabs that can then be bonded together to form full-size slabs for the 100-J Mercury aperture. Four of these slabs have been mounted onto the first set amplifier cooling vanes as shown in Figure 1.

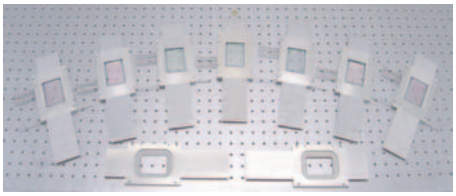

Figure 1. Gas-cooled amplifier vanes. Central three vanes are potted with surrogate Nd:Glass as placeholders until additional S-FAP slabs can be fabricated.

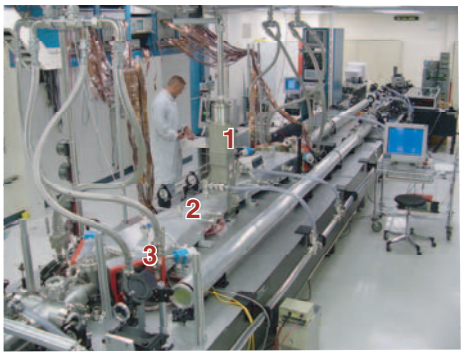

Figure 2. Mercury laboratory: (1) gas-cooled amplifier head, (2) pump delivery, and (3) diode array.

Four more slabs are in fabrication and six crystalline boules are waiting to be cut. We can anticipate having enough slabs by the end of the year to fill two amplifier cassettes. Recent measurements indicate surface damage thresholds of greater than 50 J/cm^2 when tested on a 3¥5 cm^3 sample.

The pump diodes at 900 nm, fitted with microlenses, are mounted onto etched silicon heatsinks and then mounted onto large copper blocks that provide the cooling and electrical power to the diodes. The amplifier assembly in Figure 1 was pumped by four 80-kW diode arrays. The amplifiers and pump delivery optics are shown in Figure 2 along with the diode arrays.

The system was initially operated at modest repetition rates of 0.1 Hz to avoid excessive thermal loading on the Nd:Glass slabs. With 200 mJ of front energy in a 16-ns pulse, we were able to extract up to 11.8 J of energy at 1.047 mm in a 4-pass angularly multiplexed arrangement. An energetics code was used to model the data and energy-vs-time (see Figure 3). Wavefront data was also taken for static (no pumping) and full pumping conditions. The static wavefront data show 2.7 waves of peak distortion due to bonding phase discontinuities incurred during the fabrication process. New fabrication techniques are being tested to eliminate these distortions. In the interim, a static phase corrector plate using the wet-etch technology developed by Sham Dixit and Michael Rushford of the Short-Pulse Lasers, Applications, and Technology team, was tested and shown to compensate for the distortion when placed directly adjacent to the amplifier assembly.

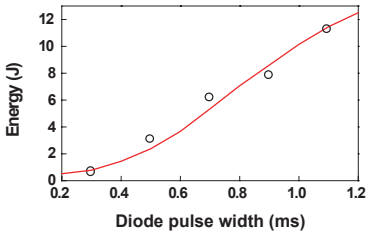

Figure 3. The energy extracted from a 4-pass S-FAP slab amplifier, using a Q-switched oscillator pulse as the seed.

Figure 4 shows the far-field spot with and without the corrector plate, indicating a factor of three improvement to reach a 2x diffraction-limited spot. The corrector plate will be used in the system until the slabs can be replaced with higher quality units.

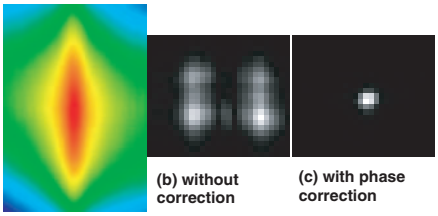

Figure 4. (a) The static wavefront of the amplifier with no diode pumping. (b) The corresponding far-field spot. (c) A phase corrector plate allows the far-field spot to reach a 2x diffraction limit.

The experimental plan is currently focused on increasing the repetition rate and injection energy to reach the next level of performance of >3 Hz and >15 J of output with the current amplifier assembly. Additional slabs are expected later in the year and will allow for full 10-Hz operation and up to 30 J of energy output with one amplifier. Activation of a second amplifier that will yield up to 100 J at 10 Hz will occur in 2003.

—C. Bibeau, A. Bayramian, K. Sculina, and S. Payne

For comments about content of the *LS&T Program Update*, contact Dr. Hao-Lin Chen (925) 422-6198.
To get on the mailing list of the *LS&T Program Update*, send a request to Helen Hoppock, hoppock1@llnl.gov
This work was performed under the auspices of the U.S. Department of Energy by
University of California Lawrence Livermore National Laboratory under Contract No. W-7405-Eng-48.

Lawrence Livermore National Laboratory
Livermore, California

PROGRAM UPDATE - AUGUST 2002

Laser Science & Technology

Dr. Lloyd A. Hackel, Program Leader

UCRL-TB-136126-02-08

Precision Optical Figuring with Wet-Etch Figuring

Wet-etch figuring (WEF) is a method for generating arbitrarily shaped optical surfaces using wet chemical etching. In WEF, the etching region on the optic is confined to a stable droplet size through the use of surface tension gradients (called Marangoni confinement), and is moved in a controlled fashion over the optic surface to precisely generate the desired optical figure on very thin glass substrates. Real-time measurement of the surface wavefront during the fabrication process and feedback allow for a closed-loop figuring operation.

Over the course of this year LS&T, with support from the Laboratory Directed Research and Development Program, has refined WEF and applied it to fabricate precision optics for a variety of applications.

Figure 1 shows a phase plate fabricated on 1-mm-thick borosilicate glass at 1.2-cm aperture, to convert a Gaussian laser beam profile to a flat-top profile at focus. The transmitted wavefront of the finished part as measured at 633 nm is shown in a false-color image as well as an interferogram. Line-outs of the focal spot intensity with and without this phase plate are also shown illustrating the Gaussian to flat-top beam shaping. This optic has been successfully used in laser machining to increase the efficiency of drilling and the quality of the drilled holes.

Figure 2 demonstrates the effects of a thin (1-mm) static phase corrector optic tailor-made to compensate for aberrations in the amplifier section of LLNL's Mercury laser. The beam aberrations were measured and were used to calculate the desired optical figure for the corrector. Interferograms of the desired and actual transmitted wavefront of the 30- x 40-mm optic are shown, along with the focal spot before and after insertion of this optic. The phase compensation allows the focal spot to approach the diffraction limit. Such phase correction optics could also be used on the National Ignition Facility (NIF) when a small focal spot is needed.

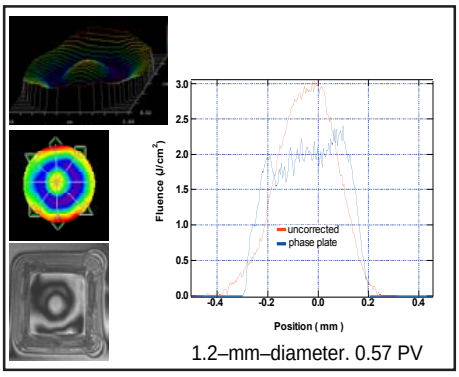

Figure 1. Contour map and interferogram of 1.2-mm-diameter beam-shaping phase plate fabricated on 1-mm-thick borosilicate glass. Also, lineout of intensity profile of laser focal spot before and after insertion of phase plate. (PV = peak-to-valley ratio.)

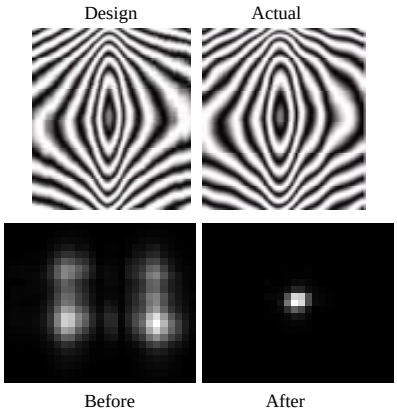

Figure 2. Design and actual transmitted wavefront interferogram of 30- x 40-mm aperture phase corrector plate fabricated for Mercury laser. Lower images show without (left) and with (right) phase plate.

We are also fabricating continuous phase plates (CPP) for the NIF laser. Figure 3 shows the desired and actual transmitted wavefronts of a 30- x 30-mm aperture CPP fabricated on a 1-mm-thick borosilicate substrate. This optic, inserted upstream in the low-power section, is designed as a beam homogenizer to generate a smooth, super-Gaussian focal spot of a desired diameter at target. The surface height gradients for this optic are 0.5 mm/mm. Some experiments can utilize these small-aperture CPPs, while others require full-apperture CPPs. Our ultimate goal is to produce these optics at full aperture.

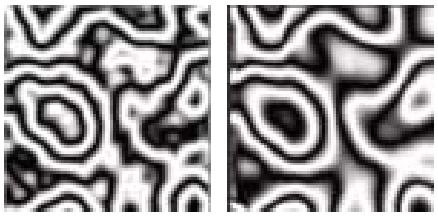

Figure 3. Design and actual transmitted wavefront interferogram of 30- x 30- x 1-mm-thick, WEF-fabricated continuous contour phase plate used for beam homogenization and spot size control for the NIF laser.

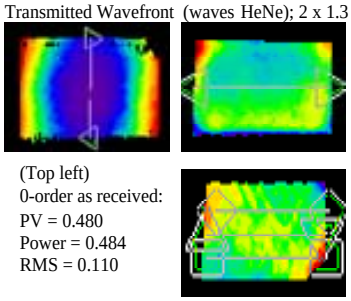

Figure 4. Transmitted zero-order wavefront of DCG grating with cover plate before and after WEF correction. Also shown is the 1st order transmitted wavefront over a 20- x 13-mm aperture. The WEF correction compensates for glue-induced distortion of this multi-element optic.

Figure 4 shows the transmitted wavefront of a multi-element, volume-phase holographic, dichromated gelatin (DCG) grating made for a telecommunication application. The DCG is sealed between two fused silica windows with optical cement. Stresses generated from the dried cement distort the overall optical figure. We used WEF to figure one surface of the optic to restore a flat transmitted wavefront. The presence of multiple interfaces and the grating layer caused multiple fringes that required a filtering algorithm to be developed to measure the true optical figure in process. We corrected the figure based on measurement of the zero-order transmitted wavefront. The first two images in this figure show the 0-order wavefront before and after WEF. The corrected optic shows an improvement to better than 10^{th} wave in power, and better than 20^{th} wave in RMS figure, with the phase distortion concentrated in one corner of the optic. The bottom plot shows that correcting the 0-order is sufficient to bring the 1^{st} order transmitted wavefront of this nominally 1-mm–period grating to an equivalent RMS value and even a better figure in terms of power.

—M. C. Rushford, S. N. Dixit, J. A. Britten, L. J. Summers, M. D. Aasen, and C. R. Hoaglan

For comments about content of the *LS&T Program Update*, contact Dr. Hao-Lin Chen (925) 422-6198.
To get on the mailing list of the *LS&T Program Update*, send a request to Helen Hoppock, hoppock1@llnl.gov
This work was performed under the auspices of the U.S. Department of Energy by
University of California Lawrence Livermore National Laboratory under Contract No. W-7405-Eng-48.

Lawrence Livermore National Laboratory
Livermore, California

PROGRAM UPDATE - SEPTEMBER 2002

Laser Science & Technology

Dr. Lloyd A. Hackel, Program Leader

UCRL-TB-136126-02-09

OSL Upgraded to 1.5 kJ

The Optical Sciences Laser (OSL) achieved an output energy of 1.5 kJ on Aug. 2, 2002, culminating an accelerated 10-month program to upgrade the laser to a kJ-class facility. Originally constructed as a 100-J, 10-cm disk amplifier system in 1990, OSL has had a distinguished history as a laser-physics test bed for the National Ignition Facility (NIF) related technologies.

OSL fielded important experiments on a variety of nonlinear optical problems including frequency conversion, optical self-focusing, stimulated optical scattering, pinhole closure, short-pulse propagation in optical fibers, and laser-induced damage of both optical and nonoptical materials. With the new capability provided by the upgrade, OSL will be able to expand its mission to include integrated testing of the NIF final optics assembly.

The upgraded laser facility, shown in Figure 1, is located in a separate room adjacent to the original OSL facility. The main element is an angularly multiplexed, double-pass Nd:glass amplifier system consisting of one 9.5-m-long vacuum relay telescope and four 20-cm amplifiers recycled from the Nova laser. Each amplifier contains three 3-cm-thick disks fabricated from NIF-surplus, platinum-free Schott LG770 laser glass. The input pulse is generated in the original OSL facility and amplified through a 5-cm rod system, after which a kinematic mirror provides a choice between further amplification in the pre-existing 10-cm system or transport to the new 20-cm system.

The pulse is injected into the 20-cm system off a small injection mirror located near the focal plane of the vacuum relay telescope, after which it passes through a spatial-filter pinhole and is collimated at a beam size of ~15 cm by the first spatial filter lens. It then undergoes two gain passes through the 20-cm amplifiers, with the second being offset in angle relative to the first to allow the pulse to miss the injection mirror and exit the amplifier system through the second lens of the relay telescope. The second telescope lens demagnifies the beam by a factor of 0.83 to allow experiments to be conducted up to the fluence limits of the transport optics without stressing the optics in the amplifier cavity.

The OSL upgrade has successfully met all 1ω performance objectives. CW gain tests have been conducted up to a maximum bank voltage of 22 kV, demonstrating a net round-trip, small-signal gain of ~900 with no evidence of parasitics. At 22 kV, and at the normal operating voltage of 20 kV, the small-signal gain coefficients for the LG770 disks are 8.5%/cm and 8.1%/cm respectively. System energetics are demonstrated in Figure 2, which plots measured output energy of the system vs the output energy of the 5-cm rod amplifier. At 20-kV bank voltage, the 1.5-kJ design energy is readily achieved at a 5-cm rod energy of 10 J (3 ns). Modeling results are also plotted for 20 and 22 kV, which show the potential for reaching output energies approaching 2 kJ.

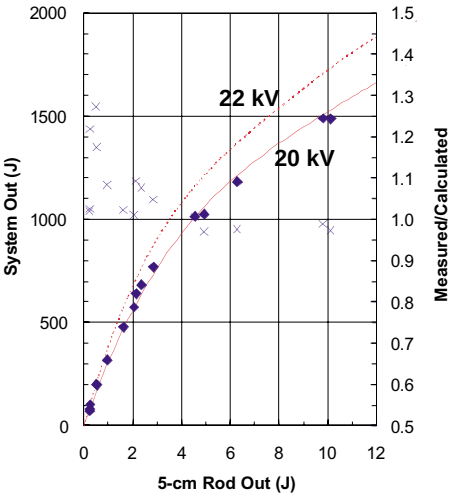

Figure 2. Plot of output energy vs injected energy (the latter measured at the output of the 5-cm rod) demonstrating operation of the system at 20-kV bank voltage up to the full design energy of 1.5 kJ.

The near-field beam quality of the system is also quite good, with measured whole-beam fluence contrasts (defined as the standard deviation of the fluence divided by the mean) of 7%. This level of beam quality is a critically important aspect of the NIF final optics test mission that will involve validating the damage resistance of 3ω optical components at NIF fluence levels. After completion of the new facility, the first-article final optics package was installed, and preparations are under way to begin experiments.

—P. Wegner, J. Caird, J. Murray, K. Skulina, S. Mills, G. Beer, T. Weiland, and D. Roberts

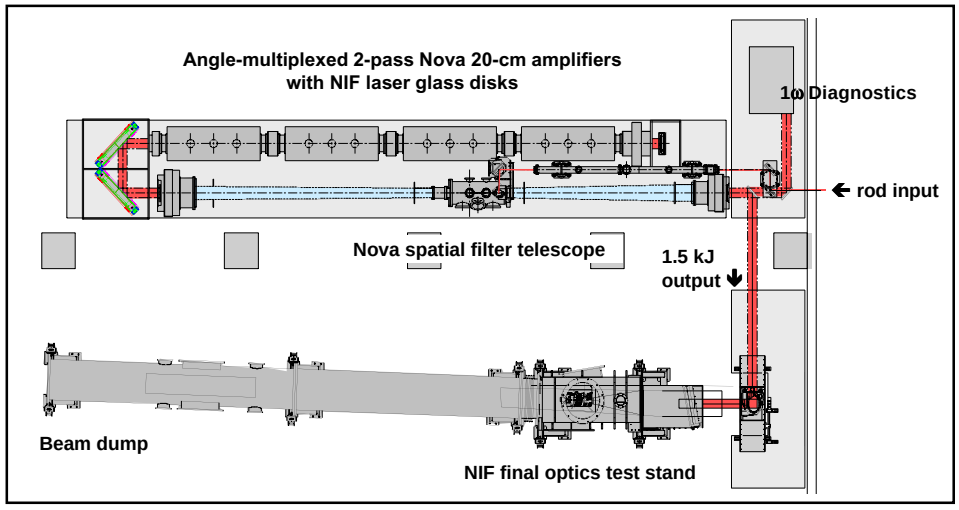

Figure 1. OSL Upgrade uses a double-pass architecture containing four 20-cm aperture disk amplifiers (twelve disks total) to deliver 1.5 kJ of 1ω energy in 3 ns for NIF final optics testing.

For comments about content of the *LS&T Program Update*, contact Dr. Hao-Lin Chen (925) 422-6198.
To get on the mailing list of the *LS&T Program Update*, send a request to Helen Hoppock, hoppock1@llnl.gov

Lawrence Livermore National Laboratory
Livermore, California

PROGRAM UPDATE - OCTOBER 2002

Laser Science & Technology

Dr. Lloyd A. Hackel, Program Leader

UCRL-TB-136126-02-10

Laser Drilling of High-Aspect-Ratio, Micron-Scale Holes for NIF Fusion Targets

One of the leading ignition target design for the National Ignition Facility (NIF) requires a capsule with a copper-doped Be ablator. Unlike plastic or glass, this material is impermeable to hydrogen, requiring that a hole be used to fill the capsule with DT fuel. The requirements for this hole are quite stringent because density perturbations in the ablator can enhance Rayleigh-Taylor instability growth during an implosion, which in turn reduces the fusion yield. Recent calculations suggest that a 3-μm-diameter straight hole would probably be acceptable.

Several technologies have been explored in the past for drilling holes of similar dimensions. These techniques include electrical discharge machining (EDM) and ion milling. The main problem encountered in these technologies is a limit in aspect ratio. For instance, EDM is able to drill through the thick material, but only if the hole is opened up to about 8 μm. Conversely, submicron-diameter holes can be made with an ion mill, but only through very thin material.

Under the support of ICF's Target Science and Technologies group, LS&T has recently built a new cutting station (Figure 1) and coupled it to an existing short-pulse machining laser. The short-pulse laser was selected to minimize the heat deposited in the area surrounding the hole and produce a sufficiently hot plasma such that the ablated material can escape the long, narrow channel.

In order to achieve the desired beam size on the front surface of the material, a high-numerical-aperture (NA) focusing system must be used. The large NA equates to a highly vergent beam into and out of the focal plane, yielding a very short depth of focus (≅1 μm). Gaussian beam propagation dictates that if the laser were focused to the diffraction-limited spot size on the front surface, the beam diameter at the exit of the capsule would be 135 μm. This is significantly larger than the size of hole required for this application.

A solution to the challenge of beam divergence is presented by the nature of the hole itself. As the hole begins to form, the walls of that hole become a metallic waveguide. This waveguide confines the propagating light in much the same way as an optical fiber.

The hole drilling system utilizes a Ti:sapphire laser that produces 1 mJ per pulse (before compression) at a 3.5-kHz repetition rate. The compressed pulse width is about 110 fs. This pulse is then spatially filtered and frequency doubled to a wavelength of 403 nm. The final available pulse energy is 1 μJ.

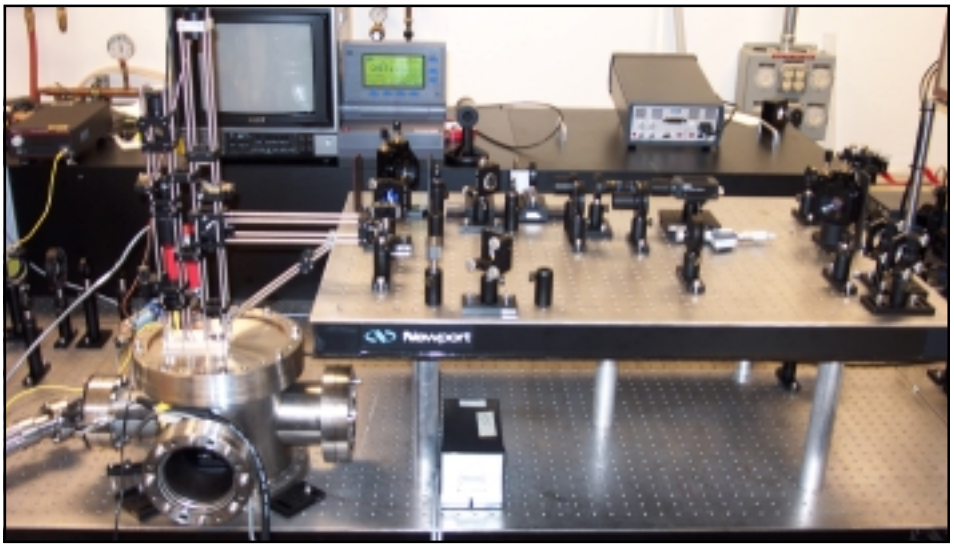

Figure 1. Cutting station for micron-scale hole drilling.

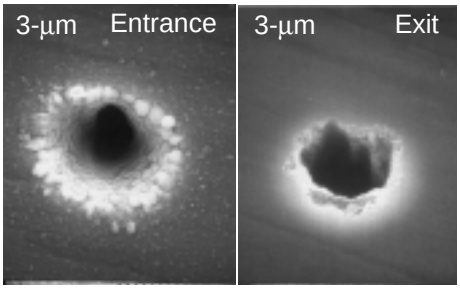

Figure 2. Laser-drilled hole through 125-μm-thick Be foil.

These laser pulses are injected into the collimated space of an infinite-conjugate-ratio microscope. The objective chosen for this project was a single-element aspheric lens with a focal length of 4 mm and a clear aperture of 4.6 mm, yielding an NA of 0.58. Due to the naturally high intensities of short-pulse lasers (about 10^{14} W/cm^2 in this application) and the small focal spot of this system, drilling must be done in vacuum. The lens is housed inside the cutting chamber and is protected from debris by a microscope cover slip.

Since the system was designed with infinite conjugates, the focal plane of the laser and the object plane of the microscope are at the same location. This allows seeing the hole as it is drilled. More importantly, it provides position feedback with sufficient resolution to reproducibly place the target precisely at focus. The microscope itself consists of a fiber-delivered laser illumination source, the aspheric objective and a 40-cm-focal-length tube lens to bring the image created by the objective to the plane of a charge-coupled device (CCD) camera. This microscope provides a field of view of about 75 μm with a resolution of 200 nm per pixel.

Early trials of the system have demonstrated the feasibility of drilling holes that extend more than 100 times beyond the system's Rayleigh range. Three-μm-diameter holes have been drilled in 125-μm-thick Be and Al foils, as well as thin-walled Be capsules. Figure 2 shows the typical entrance and exit of a hole in the Be foil.

—P. Armstrong, B. Stuart, R. McEachern

For comments about content of the *LS&T Program Update*, contact Dr. Hao-Lin Chen (925) 422-6198.
To get on the mailing list of the *LS&T Program Update*, send a request to Helen Hoppock, hoppock1@llnl.gov
This work was performed under the auspices of the U.S. Department of Energy by
University of California Lawrence Livermore National Laboratory under Contract No. W-7405-Eng-48.

Lawrence Livermore National Laboratory
Livermore, California

PROGRAM UPDATE - NOVEMBER 2002

Laser Science & Technology

Dr. Lloyd A. Hackel, Program Leader

UCRL-TB-136126-02-11

Fabrication of a 5-Meter-Diameter Diffractive Fresnel Lens

Detection and imaging of distant objects, such as the exosolar (outside our solar system) planets, require optical telescopes with large-aperture primary optics. Large apertures gather more light from these objects, thereby increasing the signal to noise. Space deployment of such telescopes severely limits the weight of the optical components and requires that the primary optic be thin, lightweight, and deployable in space.

Transmissive optics (lenses) are less sensitive to surface ripples than reflective optics (mirrors). Lenses can be made lightweight by replacing conventional lenses with diffractive Fresnel lenses. The Eyeglass project, funded by the Laboratory Directed Research & Development Program, has been developing large-aperture Fresnel lenses for space telescopes. We have built diffractive telescopes at apertures up to 50 cm diameter and demonstrated their color-corrected operation over a 470- to 700-nm-wide bandwidth.

Space deployment of large-aperture optics requires that they be packageable into a small volume for launch. In our first attempt at this, we built a 75-cm-diameter Fresnel lens (shown in Figure 1) made up of six segments and assembled using 2.5-cm-wide metal hinges. After fabrication, this lens was folded, unfolded, and was shown to produce a diffraction-limited focal spot.

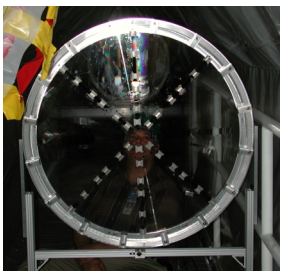

Figure 1. The 75-cm-diameter, six-panel folding lens.

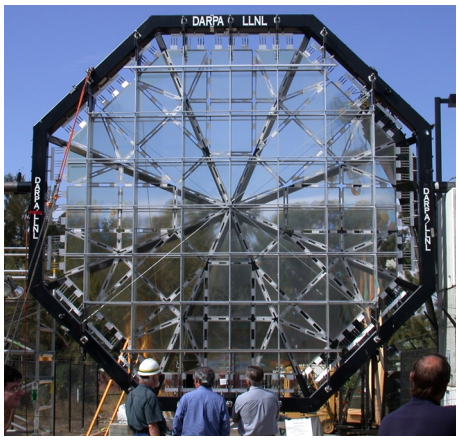

Figure 2. The 5-m Fresnel lens mounted outdoors for optical testing.

To demonstrate that this concept can be scaled up to larger sizes, we have recently built and operated a 5-m-diameter Fresnel lens (shown in Figure 2). This lens consists of 72 segments of 0.7-mm-thick glass panels that are joined together using 5-cm-wide metal hinges. The largest panel is about 600 x 770 mm in size. The particular layout of the pattern was chosen to allow the lens to be folded into a hatbox ~1/3 its size. The glass panels used for this lens are mass produced for flat-panel displays, which are inexpensive. A binary Fresnel lens pattern was applied to each panel separately using lithographic techniques. After patterning, the panels were cut to shape and the 72 pieces were glued together using a UV-curable adhesive. The assembled lens was then tension mounted in an octagonal frame and sandwiched between two metal meshes for transportation and protection against wind loading.

Optical testing of the lens consisted of hoisting the lens in a vertical position, illuminating it with monochromatic light from a laser and observing the focal spot produced by the lens. Such point-to-point tests require a minimum distance of four times the focal length between the source and the focus. We tested the lens at 405-, 532-, and 670-nm wavelengths. Figure 3a shows a focal spot produced by this lens. The focal spot size and shape are dominated by the aberrations inherent in the glass panels and the reduced precision in the alignment of the panels. Both these limitations will be overcome in the future. Figure 3b shows an image of the lens when viewed back from the focus. This confirms that light passing through the various panels reaches focus.

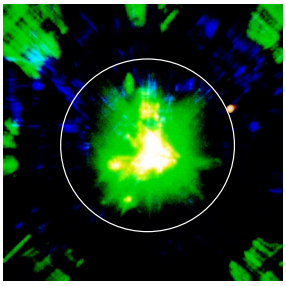

Figure 3a. Focal spot produced by the 5-m Fresnel lens when illuminated with 532-nm light. Inscribed is a 2.5-cm-diameter circle. The central portion of the image is saturated.

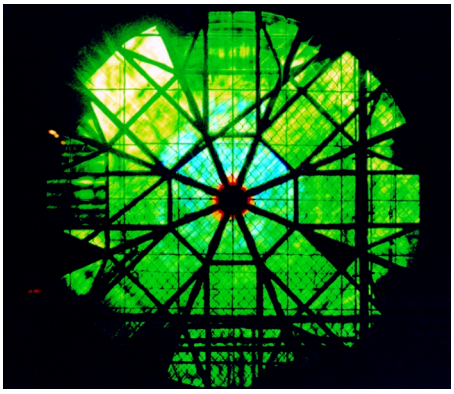

Figure 3b. View of the lens from the green-light focus.

The next phases of the project involve improving the wavefront of the panels to improve the focal-spot quality and to fabricate Fresnel lenses of even larger sizes.

—S. Dixit, R. Hyde and A. Weisberg

For comments about content of the *LS&T Program Update*, contact Dr. Hao-Lin Chen (925) 422-6198.
To get on the mailing list of the *LS&T Program Update*, send a request to Helen Hoppock, hoppock1@llnl.gov
This work was performed under the auspices of the U.S. Department of Energy by
University of California Lawrence Livermore National Laboratory under Contract No. W-7405-Eng-48.

Lawrence Livermore National Laboratory
Livermore, California

PROGRAM UPDATE - DECEMBER 2002

Laser Science & Technology

Dr. Lloyd A. Hackel, Program Leader

UCRL-TB-136126-02-12

Diode-Pumped Nd:GGG Laser—First Light

Under the support of the U.S. Army's Space and Missile Defense Command, and in collaboration with industrial partners including Decade Optical Systems (DOS), Northrop/Grumman, and others, we are developing high-average–power (100-kW–class), diode-pumped solid-state, heat-capacity laser technology for applications in tactical short-range air defense missions.

As a proof-of-principle, we have built and delivered a 10-kW–class (13 kW actual) heat-capacity laser to White Sands Missile Range. This laser employed flashlamp pumping of the Nd:glass laser slabs. But to advance to a 100-kW–class laser, laser-diode pumping will be used for increased power and efficiency, and crystalline laser media for better thermal characteristics. The baseline design for such a laser uses Nd:doped gallium gadolinium garnet (GGG) as the laser medium and laser-diode pumping at 808 nm.

To establish a solid technical basis for such a laser, we have developed a half-scale testbed that utilizes a single Nd:GGG slab with an active region measuring 5 x 10 cm^2 in size and is pumped by four half-size laser diode arrays. A schematic of the laser is shown in Figure 1. The diode arrays consist of 28 SiMM (Silicon Monolithic Microchannel) "tiles" arranged in a 4x7 configuration and produce an average optical power of 4.2 kW/array. The pulse width is nominally 500 μs.

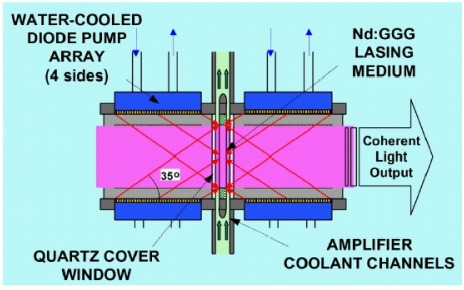

Figure 1. Schematic of the pump cavity. This is the fundamental building block of the diode-pumped Nd:GGG laser system.

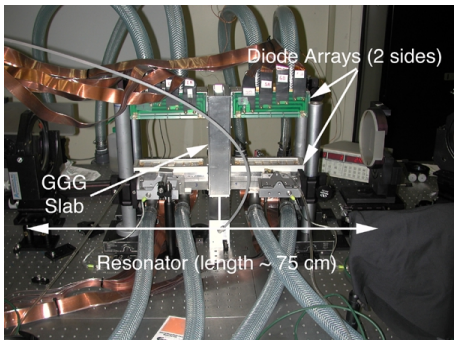

Figure 2. Photo of the half-size-slab experiment.

Figure 2 shows the experimental setup of the half-scale heat-capacity laser. In the middle, one can see the slab holder with the four pump arrays surrounding it. The entire laser system is extremely compact—the diode arrays shown are roughly 6 in. long and the entire cavity is only 75 cm long. We performed a series of experiments to verify the performance of this new laser. Optical gain coefficient, pump uniformity, output wavefront, and temperature rise in the lasing medium were measured to benchmark our temperature-dependent energetic model.

Using a stable resonator with low-output coupling, we obtained kW output from the half-scale system. At 200 Hz, over a ten-second run, we achieved an average power of 2.7 kW with an initial output in excess of 3 kW. The cavity consisted of a flat high reflector and an 85% reflectivity concave output coupler with a 10-m radius of curvature. No attempt was made to optimize either the output reflectivity or the curvature of the reflectors. Figure 3 shows a typical high-energy pulse from this system.

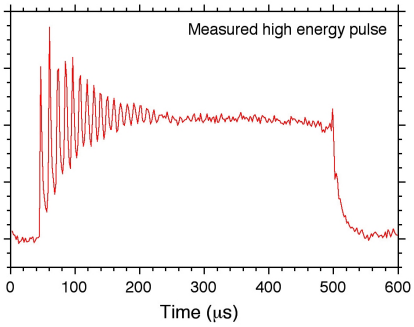

Figure 3. Typical laser output pulse, showing the presence of relaxation oscillations at the beginning of the pulse.

Figure 4. Frame taken from a movie showing the interaction of the laser beam with a steel coupon. The beam has punched through the coupon at this point.

The average diode-array optical pump power used for this experiment was 13.3 kW and the overall diode electrical efficiency was 45%. Thus, the total electrical efficiency of the half-scale slab laser works is ~9%, a figure very near the 10% goal designed for the 100-kW mobile laser system. Using the output beam, we were able to penetrate a 1.5-mm-thick steel coupon in a matter of a few seconds (Figure 4).

In fiscal year 2003, we plan to activate the three-slab diode-pumped Nd:GGG testbed as a scientific prototype for the 100-kW system to be developed for battlefield defense. It is anticipated that this system will generate an output power in excess of 15 kW—greater than the nine-slab flashlamp-pumped system currently in operation at the Army's High Energy Laser Systems Test Facility (HELSTF).

—M. Rotter and S. Mitchell

For comments about content of the *LS&T Program Update*, contact Dr. Hao-Lin Chen (925) 422-6198.
To get on the mailing list of the *LS&T Program Update*, send a request to Helen Hoppock, hoppock1@llnl.gov
This work was performed under the auspices of the U.S. Department of Energy by
University of California Lawrence Livermore National Laboratory under Contract No. W-7405-Eng-48.